

TriboPump: A Low-Cost, Hand-Powered Water Disinfection System

Wenbo Ding, Jianfeng Zhou, Jia Cheng, Zhaozheng Wang, Hengyu Guo, Changsheng Wu, Sixing Xu, Zhiyi Wu, Xing Xie,* and Zhong Lin Wang*

Water disinfection at the point of use (POU) has enormous social and economic significance, especially for rural areas or catastrophes. To tackle the requirements of power independence and cost control in such applications, the concept of TriboPump is proposed, which is a low-cost, hand-powered water disinfection system. The system consists of three functional parts: a tubular coaxial-electrode copper ionization cell (CECIC) as the disinfection device, a disk triboelectric nanogenerator (D-TENG) as the power source, and a coaxial mechanical structure including the water pump. The adoption of D-TENG can make the system adaptive to varying system resistances without additional power management circuits. Moreover, the integration of CECIC and TENG can successfully turn their intrinsic limitations into advantages and a synergic effect is achieved. With the integrated design, the system can effectively disinfect the water while pumping it solely by hand power. The cost estimate of the whole system can be as low as \$10 for a 2-year service. It is believed that the whole system design provides a feasible one-stop and cost-efficient solution for POU water pumping and disinfection, which will ideally be suitable for rural areas or sudden-onset catastrophes.

1. Introduction

Water covers 71% of the earth's surface. However, there is 1 out of 9 people in the world who still has no direct access to clean water due to pathogen contamination, according to the World Health Organization's (WHO's) report in 2017.^[1] The situation is exacerbated by factors such as the secondary contamination during water distribution,^[2] the breakdown of centralized facilities under natural disasters or wars,^[3] or the most likely one which is the unaffordable capital cost for large water treatment plants in rural areas.^[4] In this context, the water disinfection techniques at the point of use (POU) have attracted tremendous interests from both academia and industry, which are of enormous social and economic significance.^[5,6]

The POU water disinfection is a cost-effective mobile complement to the traditional centralized approach, especially in the extreme cases where only a small portion of water needs to be treated for drinking purpose. The most widely used POU disinfection methods include chlorination,^[7] ultraviolet radiation,^[8] and membrane filtration.^[9] Assisted by engineered nanomaterials,^[10,11] the photocatalytic,^[12] electrochemistry,^[13] low-voltage electroporation,^[14] and microwave^[15] based disinfection methods have been developed and shown great potential for POU purposes. Nevertheless, these methods have their own pros and cons, which need careful choosing and customized optimization for specific application scenarios. For example, the performance of the photocatalytic water disinfection is always confined by the raw water turbidity.^[16] Low-voltage electroporation disinfection achieves superior results, but durable electrode materials are still in development.^[14] Electrochemical disinfection is also of great interests because of its versatile nature.^[17] However, the extensive energy consumption limits the commercialization.^[18] For the possible deployment in developing areas or catastrophes, there are two key requirements that need to be considered when designing the POU water disinfection equipment, i.e., the least dependence of electrical power supply and the best possible performance with relatively low cost.^[19]

The triboelectric nanogenerator (TENG) invented by Wang and co-workers in 2012 is an emerging mechanical energy harvesting mechanism, which can effectively harness the


Dr. W. Ding, Dr. H. Guo, Dr. C. Wu, S. Xu, Dr. Z. Wu, Prof. Z. L. Wang
School of Materials Science and Engineering
Georgia Institute of Technology
Atlanta, GA 30332, USA
E-mail: zhong.wang@mse.gatech.edu

J. Zhou, Prof. X. Xie
School of Civil and Environmental Engineering
Georgia Institute of Technology
Atlanta, GA 30332, USA
E-mail: xing.xie@ce.gatech.edu

Prof. J. Cheng, Z. Wang
State Key Laboratory of Tribology
Department of Mechanical Engineering
Tsinghua University
Beijing 100084, China

Prof. Z. L. Wang
Beijing Institute of Nanoenergy and Nanosystems
Chinese Academy of Sciences
Beijing 100083, P. R. China

Prof. Z. L. Wang
School of Nanoscience and Technology
University of Chinese Academy of Sciences
Beijing 100049, P. R. China

 The ORCID identification number(s) for the author(s) of this article can be found under <https://doi.org/10.1002/aenm.201901320>.

DOI: 10.1002/aenm.201901320

kinetic or ambient energy.^[20] Due to its advantages including broad material availability, light weight, low cost, high voltage output, and high efficiency for low frequency stimuli, the TENG has been successfully deployed in numerous application scenarios, such as blue energy harvesting,^[21] wearable devices,^[22] Internet of things devices,^[23] human machine interfaces,^[24] mass spectrometer,^[25] and microplasma.^[26] Recently, there are also some interesting works on the environmental applications of TENGs, mainly on air purification,^[27,28] heavy metal and dye removal,^[29] anti-biofouling,^[30–32] and so on. Nevertheless, there is no systematic study on the disinfection performance of TENGs or one-stop design of the TENG driven POU water disinfection solution.

In this paper, we propose the concept and implementation of a low-cost and hand-powered pump with the function of water disinfection based on the TENG, henceforth referred to as TriboPump. The TriboPump consists of three main parts, a tubular coaxial-electrode copper (Cu) ionization cell (CECIC) as the disinfection device, a disk TENG (D-TENG) as the power source, and a coaxial mechanical structure including the water pump. We demonstrate that the proposed design can pump and disinfect the water with no need of additional complicated circuits. The main contributions of this paper can be fourfold.

First, the coaxial mechanical structure design and the integration into a 3D printed support with a well-matched gear ratio make the D-TENG and water pump able to be driven by the same rotating mechanical stimuli (e.g., hand power) while achieving different rotate speeds.

Second, the D-TENG will work on the near-short-circuit (impedance-mismatching) regime so that it can have the constant current output under different loads, which makes it adaptive to different water qualities without additional complicated power management circuits.

Third, the novel CECIC has a simple design but can have a good disinfection performance while ensuring a low Cu release concentration. Together with the mechanical design, the whole system can be effectively operated by hand power and have a low cost which is as low as \$10 for a 2-year service in a single family.

Fourth, either the CECIC or the TENG has its own limitations when being separately applied in practice. By integrating them together, their shortcomings are turned into advantages and a synergic effect is achieved.

We believe that the whole system design provides a feasible one-stop and cost-efficient solution for POU water pumping and disinfection, which will be ideally suitable for the rural areas or sudden-onset catastrophes without direct access to power supply.

2. System Design

The systematic concept of the TriboPump is described in Figure 1a, where the bacteria in the water will be inactivated

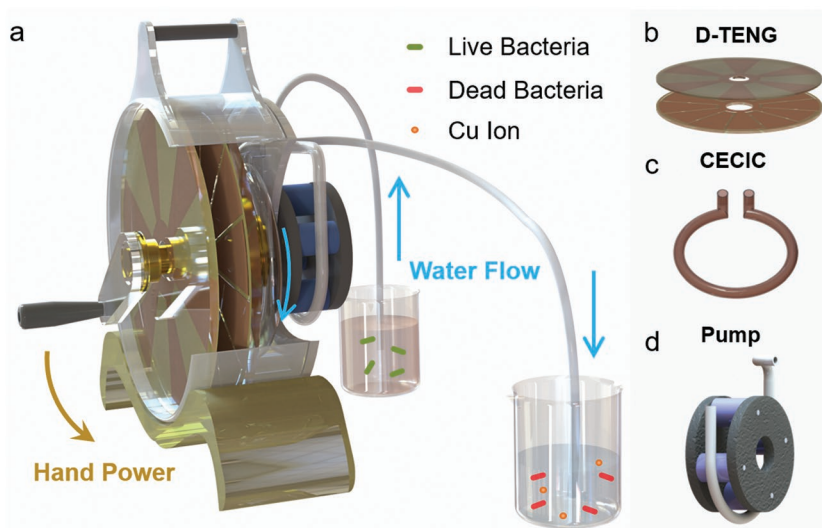


Figure 1. The conceptual schematic of the proposed TriboPump. a) The schematic diagram of the whole system. b) The schematic diagram of the D-TENG part. c) The schematic diagram of the CECIC part. d) The schematic diagram of the water pump part.

during the water pumping process and the whole system can be operated solely by hand power. The whole system consists of three functional parts, i.e., the CECIC as the disinfection device, the D-TENG as the power source, and the coaxial mechanical structure including the water pump, as illustrated in Figure 1b–d.

2.1. CECIC as the Disinfection Device

For better deployment in rural areas, many key factors need to be taken into consideration when designing the disinfection device, such as low cost, high robustness, and good performance. To this end, we adopt the CECIC as the disinfection part in this design.^[33] As demonstrated in Figure 2a,b, the device is composed of a tubular disinfection chamber and a reactor holder for assembling. It should be noted that in the final system design, the chamber will be embedded to the pump structure and the reactor holder which is space-consuming will be no longer needed. The disinfection chamber has a sleeve-tube structure with two electrodes, i.e., the outer and the center ones. The outer electrode is made of a rolled Cu foil adhered on the inner surface of the tube, and wired to the negative output of the power source. The center electrode is a coaxial thin Cu wire in the center of the chamber and is connected to the positive electrode of the power source.

The CECIC has achieved high removal efficiency of *Escherichia coli* (≈ 6 logs) with a direct-current (DC) voltage in deionized (DI) water. Actually, there are multiple mechanisms involved in the disinfection process of the CECIC, which synergistically contribute to the efficient pathogen inactivation. First, the Cu ions are considered to be the primary disinfectant. When the external power source is applied, the Cu ions are in situ released from the center electrode, which creates a Cu ion concentration gradient along the radial cross section of the reactor. The Cu ion concentration within 0.05 cm

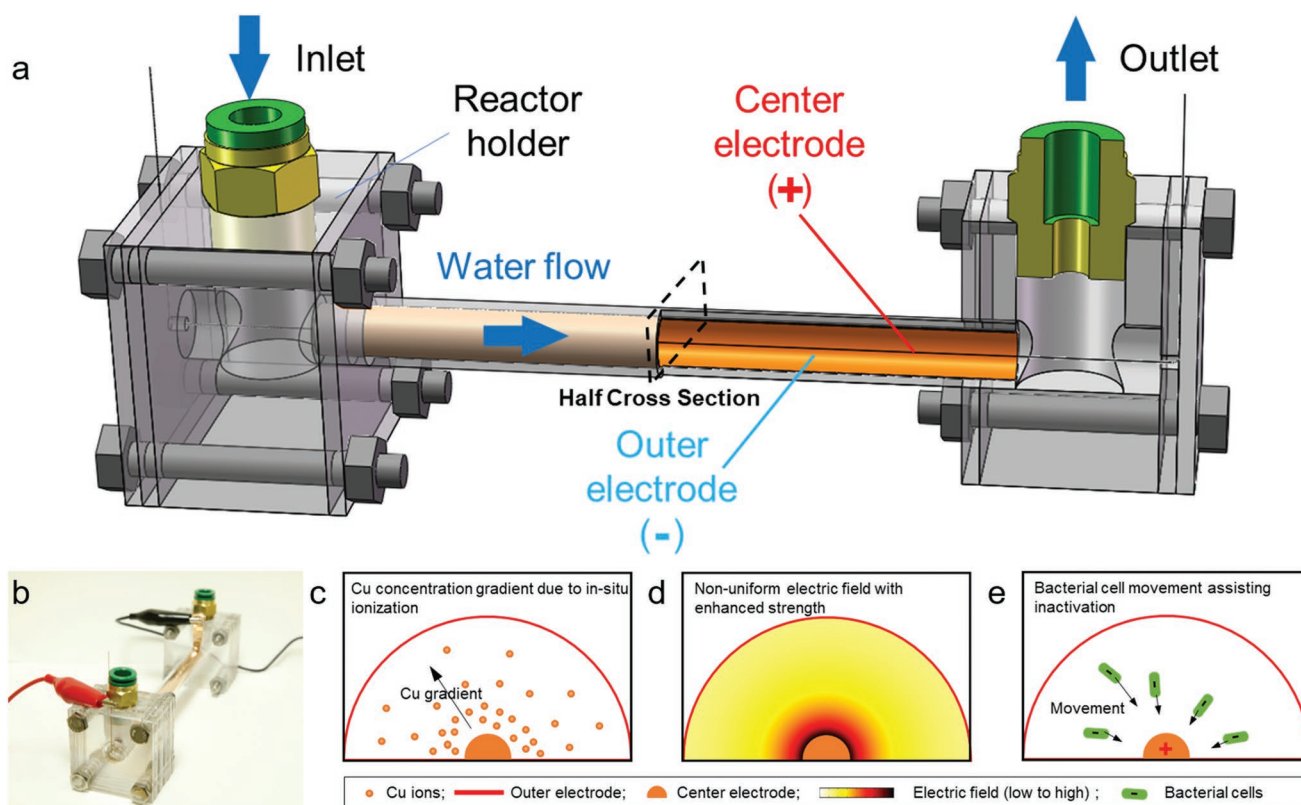


Figure 2. An overview illustration of the coaxial-electrode copper ionization cell (CECIC) and its disinfection mechanisms. a) The device structure and the component parts of CECIC. b) Demonstration of the CECIC for experiments. c) The schematic diagram of the Cu ion concentration gradient due to the in situ ionization (half cross section). d) The electric field distribution profile inside the tubular disinfection chamber of the reactor simulated by COMSOL (half cross section). e) The schematic diagram of the bacterial cell movement assisting inactivation (half cross section).

from the center electrode is more than ten times higher than the bulk concentration, as described in Figure 2c. Second, the enhanced electric field increases the permeability of the bacterial cell membrane, and thus enhances the Cu consumption into the bacterial cells. The rational designed coaxial configuration enables an electric field strength of $>80 \text{ V cm}^{-1}$ near the center electrode with an applied DC voltage of 1.5 V, which is 26 times higher than that of a conventional planar-electrode system, as illustrated in Figure 2d. Third, the nonuniform electric field assisted disinfection by transporting bacteria to the adjacency of the center electrode, where there is both higher copper concentration and electric field strength. Two forces are involved in the bacterial transportation, which are electrophoresis and dielectrophoretic forces, as depicted in Figure 2e. The negatively charged bacterial cells subjected to the electrophoresis force move against the electric field, which points to the center electrode. Meanwhile, the dielectrophoretic force also moves dielectric particles (i.e., the cells) to the center electrode in such a nonuniform electric field. With all the mechanisms mentioned above working together, the CECIC can achieve a satisfactory inactivation efficiency (>6 -log inactivation of *E. coli*) with only $\approx 200 \mu\text{g L}^{-1}$ Cu ion concentration release, which is superior to the existing methods and far below the maximum contaminant level goal (MCLG) of Cu for drinking water (1.3 mg L^{-1}) set by the United States Environmental Protection Agency.

2.2. D-TENG as the Power Source

The typical water pump usually has a rotary structure driven by the mechanical stimuli. To fully utilize the mechanical stimuli and produce electricity for water disinfection, a disk structure is adopted for the TENG design and shares the common axis with the mechanical water pump, as illustrated in Figure 1a. The D-TENG used in the design consists of two main parts, i.e., the stator and the rotator, which both have the radial patterns and are fabricated via the printed circuit board (PCB) techniques, as depicted in Figure S1 in the Supporting Information. The stator has 120 Cu radial sectors with each central angle of 1.5° and length of 83 mm, which are connected to two electrodes and form a complementary pattern. The whole stator is covered by a layer of the polytetrafluoroethylene (PTFE) film with a thickness of $100 \mu\text{m}$ as the triboelectric material. Similarly, there are 60 Cu radial sectors with each central angle of 1.5° and length of 83 mm at the rotator, which work as the inductive conductor. The Cu of the rotator is first printed on the soft substrate with the help of soft and flexible PCB techniques and then attached to a rigid acrylic substrate with a thickness of 5 mm. In this way, the intimate contact between the stator and rotator can be ensured and thus the triboelectrification performance will be enhanced when operating. Thanks to the simple structure and mature PCB techniques, the D-TENG can achieve a satisfactory performance as well as robustness with relatively low costs.

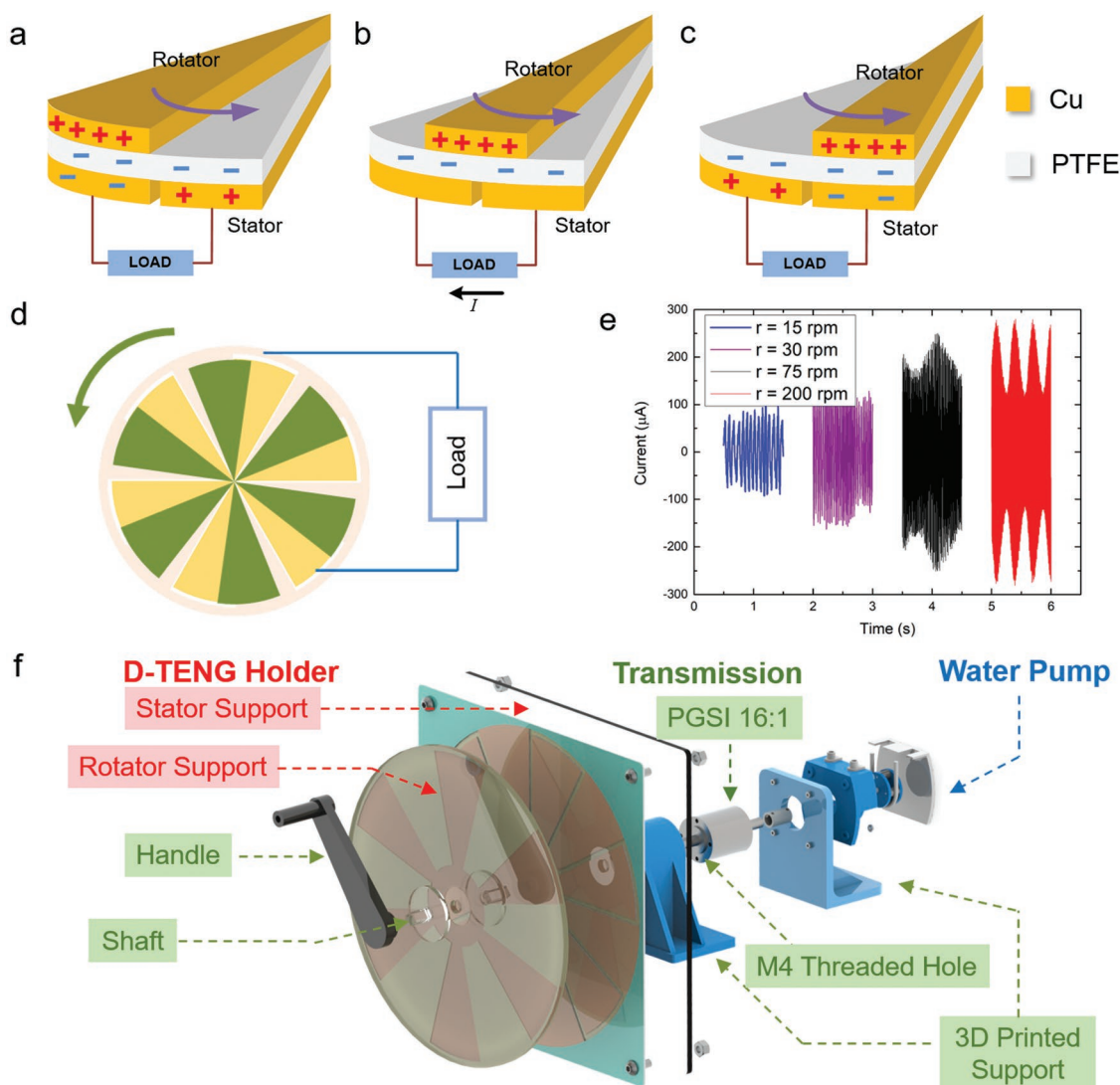


Figure 3. The integrated design of the D-TENG and the mechanical water pump. a–c) Schematics for the working mechanism of the D-TENG. d) The equivalent working model of the D-TENG with external loads. e) The output short-circuit currents of the D-TENG under different rotate speeds. f) The explosive view of the coaxial mechanical design demonstrating the transmission details.

Detailed fabrication process and parameters are discussed in Note S1 in the Supporting Information.

Generally speaking, the working mechanism of the TENG is based on the coupling effect of the triboelectrification and electrostatic induction.^[34] In this case, because of different triboelectric polarities of the two triboelectric surfaces, positive and negative electric charges are created on the Cu surface of the rotator and PTFE surface of the stator respectively after several cycles of friction. Subject to the law of charge conservation, the density of positive charges on the rotator is twice as much as that of negative ones on the stator because of unequal contact surface area of the two objects. When there is the load connected to the two output electrodes of the stator, the electrical current will be generated due to the redistribution of the free charges between the two electrodes when the rotator rotates periodically. For brevity, a basic unit is used for elaborating the process, as illustrated in **Figure 3a–c**, and the equivalent

working model of the D-TENG is demonstrated in **Figure 3d**. Due to the miniaturizing and integrating of the electrodes, the D-TENG has the advantages of a relatively high current. As depicted in **Figure 3e**, the short-circuit current output will increase with the rotate speed going up. If being driven by the normal hand power, for example, under 30 revolutions per minute (rpm) and 75 rpm, the short-circuit current could have an average of 100 and 150 μA , respectively, which is consistent with the previous study.^[34]

2.3. Coaxial Mechanical Structure with Water Pump

The coaxial mechanical structure including the water pump in this design can be divided into three parts, as demonstrated in **Figure 3f**. The first part is the D-TENG holder: The stator of D-TENG is adhered with an acrylic plate

($300 \times 300 \times 5 \text{ mm}^3$) with mounting holes through which the stator is fixed to the 3D printed support made of the polylactic acid (PLA) material. A foldable handle is connected to the rotator of D-TENG. The second part is the transmission of the entire device. Since the D-TENG and water pump are driven by the same stimuli, there must be an optimized rotate speed ratio between them to guarantee the disinfection effect. In order to achieve an ideal match between the rotate speeds of the TENG (20–60 rpm) and pump (320–960 rpm), and minimize the size of the whole device at the same time, the planetary gear speed increaser (PGSI, the speed increase ratio is 16:1, the total diameter is 42 mm, the total length is 100 mm, and the input-and-output shaft is $\varnothing 10 \text{ mm}$) is selected as an intermediate transmission component. The end face of the PGSI has four M4 threaded holes distributed around the wheel, through which the PGSI can be fixed on the support, similar to the stator of D-TENG. At the same time, the rotator of the D-TENG is fixed to the input shaft of the PGSI via a flange. The third part is the water pump: it adopts micro-peristaltic water pump (Model KCM-S-14-4) produced by Kamoer company. The liquid in the pump tube is not directly contacted with the pump body which can prevent secondary contamination of the liquid in the pump. The rotating part of the pump consists of four small rotors. The outer diameter of the peristaltic silicone tube is 4.8 mm, and the inner one is 1.6 mm. The measured flow rate of the water pump under the typical input stimuli of the system (960 rpm) is around 60 mL min^{-1} and can be easily lowered to a proper value by controlling the valve according to the system requirements. The water pump is fixed on the support through the four M3 threaded holes on the pump mounting plate. The input shaft diameter of the pump is 5 mm, which is connected to the output shaft of the PGSI with a coupling ($\varnothing 5\text{--}10 \text{ mm}$).

3. Results

In this section, we will study the equivalent working model of the TriboPump and provide the disinfection performance of the system prototype. Based on the previous study on the electric field assisted water disinfection, the DC power source has superior performance than the alternating current (AC) one.^[33] Thus, in the proposed system, the output of the D-TENG is connected to a rectifier bridge for the AC-to-DC conversion, and a paralleled capacitor is also adopted to suppress the current fluctuation in the external load. The equivalent circuit of the TriboPump under working mode is illustrated in **Figure 4a**, where the D-TENG is modeled to be the series connection of a voltage source V and an inner capacitor C_p , the paralleled capacitor has the capacitance of C_p , and the reactor has the resistance of R . The current waveforms in the load under different load resistances are measured and shown in **Figure S2** (Supporting Information), where the paralleled capacitance is $C_p = 10 \mu\text{F}$ and the rotate speed of the stimuli is 60 rpm similar to that of the human operation. It can be seen from **Figure S2** (Supporting Information) that the current will become more similar to DC current when the resistance increases, and such effects can be achieved as well by increasing the paralleled capacitance. Moreover, we

have studied the influences of the water quality and flow rate on the reactor resistance, as illustrated in **Figure 4b**. Here the flow rate is represented by hydraulic retention times (HRT, $\text{HRT} = \text{Device effective volume}/\text{Flow rate}$) and the river water is collected from the Chattahoochee River in Atlanta, of which the detailed characteristics are provided in Note S2 and **Figure S3** in the Supporting Information. According to different conditions, the reactor resistance may vary from several to tens of $\text{k}\Omega$. The current magnitudes flowing through the external load with different paralleled capacitors are simulated based on the equivalent model, as depicted in **Figure 4c**. The detailed calculation can be found in Note S3 in the Supporting Information. The simulated results have revealed a unique feature of the TENG that there is a near-short-circuit regime (impedance-mismatching, the external load is lower than a certain level) where the output current could remain relatively unchanged regardless of the load resistance. Such feature is mainly due to the large intrinsic impedance of the TENG, and was considered to be a disadvantage when the TENG is used to power commercial electronics. Fortunately, we have taken advantage of such feature to skillfully solve the varying resistance issue of CECIC, which could avoid the complicated power management circuit and further lower the costs. The corresponding experiments are carried out, and the results are consistent with the simulations, as illustrated in **Figure 4d**. The output current of the DC voltage source is also measured under different resistances, and it can be seen that the performance is severely influenced by the external load. Nevertheless, the output current of the D-TENG remains almost unchanged within the grey zone indicating the resistance range of the reactor (see **Figure 4b**), which suggests that a more stable disinfection performance is guaranteed.

Water disinfection experiments were carried out to evaluate the performance of D-TENG driven CECIC. Water sample containing $\approx 10^7$ colony-forming units (CFU)/mL bacteria flowed through the reactor with various HRTs (0.5–5 min, corresponded to the flow rates of $20\text{--}2 \text{ mL min}^{-1}$). The D-TENG was driven by a linear rotary motor (Baldor Reliance Industrial Motor, CDP3450) with the rotate speed set to 60 rpm which mimics the hand power input, and had an estimated current output with the root mean square (RMS) value of around $80 \mu\text{A}$. The experimental system setup is illustrated in Note S4 and **Figure S4** in the Supporting Information. The circuit configuration follows the schematic in **Figure 4a**. Four strains of bacteria were used as indicators, including *E. coli* (gram negative), *Enterobacter hormaechei* (gram negative), *Bacillus subtilis subsp. Subtilis* (gram positive), and *Staphylococcus epidermidis* (gram positive). As shown in **Figure 5a–d**, the inactivation efficiencies general increase with the increase of the HRTs. When the HRT is higher than 2.5 min, the inactivation efficiencies achieved ≈ 6 logs and no live bacteria were detected in the effluent. Standard spreading technique was applied to quantify the concentration of the bacteria. The plating results (Insets of **Figure 5a–d**) show a comparison between a complete bacterial inactivation by the TriboPump (right) and control groups that no treatment (left) was taken. The detailed measurement process of the bacteria inactivation efficiency is provided in Note S5 in the Supporting Information. The effluent Cu concentration was also measured as an indicator of the health risks, as shown in **Figure 5a**. Generally, the longer

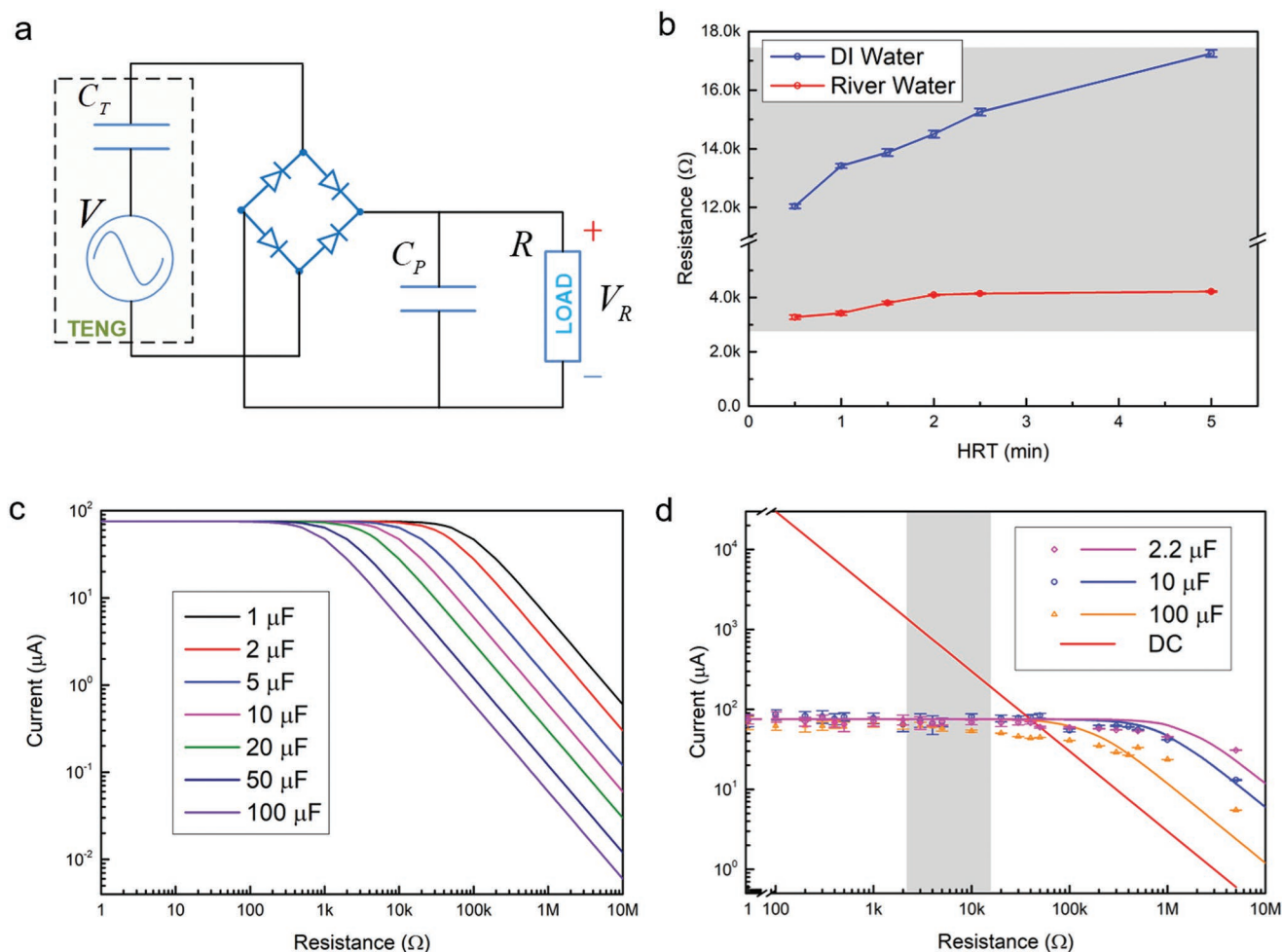


Figure 4. The systematic study on the equivalent model of the TriboPump. a) The equivalent circuit model of the TriboPump under working mode. b) The measured reactor resistances with DI water and river water under different flow rates. c) Simulation results of the current magnitude flowing through the external load with different paralleled capacitors. d) Experiment results and fitted curves of the measured current magnitude flowing through the external load with different paralleled capacitors.

HRT results in a higher Cu concentration in the effluent. When the HRT is between 2.5 and 5 min, the Cu concentration is around $180\text{--}340\ \mu\text{g L}^{-1}$ which is far below the MCLG of $1.3\ \text{mg L}^{-1}$, and meanwhile high inactivation efficiencies (≈ 6 logs) are achieved.

The Movie S1 (Supporting Information) demonstrates the prototype of the TriboPump and its operation by the hand power. For the future practical products, the reactor will be integrated into the TriboPump and the space-consuming reactor hold could no longer be needed after careful structural design. Moreover, the cost estimate of the TriboPump is calculated in Note S6 (Supporting Information), and the total cost of the whole system including capital and operation costs can be as low as \$10 for a 2-year service.^[35]

4. Conclusion

Honestly speaking, either the CECIC or the TENG has its own bottlenecks when being separately applied in practice. For the

CECIC, on one hand, the electricity dependence will limit its deployment in rural areas or catastrophes where the power grid or battery is not accessible. On the other hand, unlike the ideal experimental conditions, the actual system resistance of the CECIC varies due to the different water quality, flow rate, temperature, reactor volume, etc. To guarantee a stable Cu ion release, a constant current will be required, leading to additional costs on the control circuit. For the TENG, it has a very unique characteristic which is of a high voltage but low current output, exhibiting a large inner impedance and thus nonideal as the power source for commercial electronics. Normally, this issue can be addressed by adding a power management circuit and matching the load impedance, which is not cost-effective. Fortunately, in this design, we take advantage of this unique feature by having the CECIC work at the near-short-circuit (impedance-mismatching) regime of the TENG and hence could significantly simplify the power management circuit. Besides, the coaxial structural design can make the CECIC and TENG driven by the same rotating stimuli. That is to say, by integrating the CECIC and TENG together, their

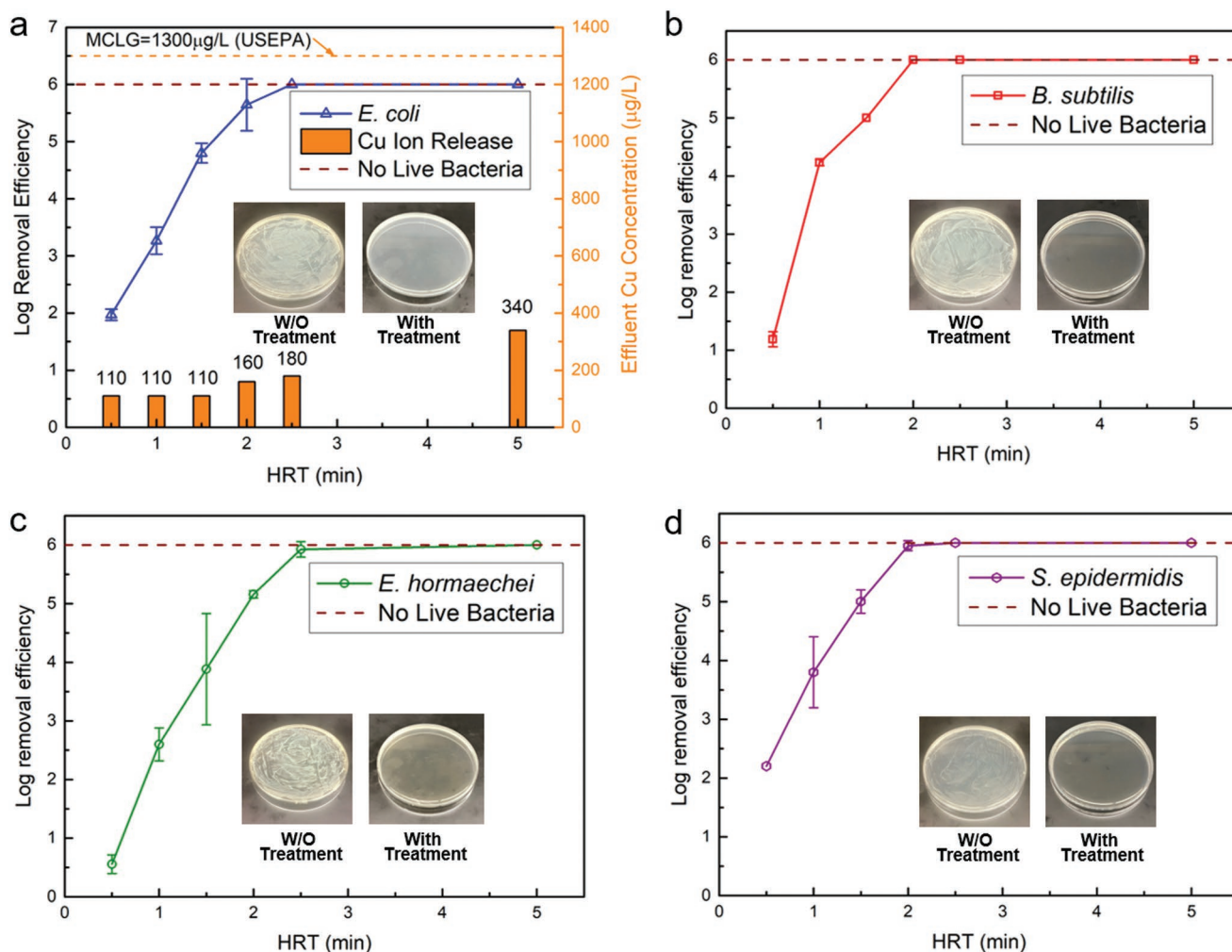


Figure 5. The system implementation and disinfection experiment results. a) The disinfection results of TriboPump for *E. coli* under different flow rates and the corresponding effluent Cu concentration. b) The disinfection results of TriboPump for *B. subtilis*. c) The disinfection results of TriboPump for *E. hormaechei*. d) The disinfection results of TriboPump for *S. epidermidis*.

shortcomings are turned into advantages and we kill two birds with one stone.

To summarize, in this paper, we propose the concept and implementation of the TriboPump system, which consists of three parts, a tubular CECIC as the disinfection device, a D-TENG as the power source and a coaxial mechanical structure including the water pump. The coaxial design and the integration into a 3D printed support with a well-matched gear ratio enable the D-TENG and water pump to be driven by the same rotating stimuli. The unique characteristic of TENG that has large inner impedance is directly utilized to deliver constant currents under different reactor resistances, resulting in a significant simplification in the power management. The novel CECIC disinfection device has a simple structure and low cost while maintaining an acceptable performance. The whole system can be easily operated by hand drive and provides a feasible one-stop and cost-efficient solution for POU water pumping and disinfection, which will be ideally suitable for the rural areas or sudden-onset catastrophes.

5. Experimental Section

Circuit and Measurement of Electric Characteristics: The output current of the D-TENG was monitored and measured through the programmable electrometer (Keithley 6514). The measurement signals were recorded via the high-speed data acquisition (DAQ) system (National Instrument DAQ) under the control of LabView 2016 (National Instrument).

Fabrication of the CECIC: The tubular-shape CECIC consisted of one cylindrical treatment chamber in the middle and two tube fitting modules on both sides serving as the inlet and outlet. The treatment chamber was made by an acrylic round tube (McMaster-Carr, 0.95 cm inner diameter) with a total length of 13.8 cm. A cylindrical copper shim (McMaster-Carr, 152 µm thick) was used to cover the whole internal surface of the tube, serving as the outer negative electrode. A Cu wire (McMaster-Carr, 110 copper) was hung in the center along the tube, serving as the coaxial center positive electrode. The diameter of the copper wire was 76 µm. A platinum wire (Alfa Aesar, type R thermocouple) with the same diameter (76 µm) was used in the control experiments. The effective volume of the CECIC was 10 mL. The acrylic reactor holder was fabricated using the laser cutter machine (Universal VLS 6.60 60W CO₂ laser) and automatic mill machine (Green TRAK K3 Mill) in the Biomedical Engineering Design Shop at Georgia Institute of Technology.

Measurement of Cu Concentration: The Cu concentration was measured by the porphyrin method using the Cu Test Kit (HACH, porphyrin method 8143) and following the vendor's manual. Some samples were filtered through 0.45 μm syringe filters to remove the suspended *E. coli* cells so that the concentrations of the total Cu, the dissolved Cu ions in the solution, and the Cu adsorbed or taken by the cells can be determined.

Measurement of Bacteria log Removal Efficiency: The details can be found in Note S5 in the Supporting Information.

Supporting Information

Supporting Information is available from the Wiley Online Library or from the author.

Acknowledgements

W.D., J.Z., and J.C. contributed equally to this research. W.D. and Z.L.W. conceived the idea. W.D. designed the whole concept, the system functionality and the D-TENG part. J.Z. designed the CECIC and conducted the disinfection experiment. J.C. designed the mechanical water pump and the 3D printed support. Z.W. fabricated and implement the mechanical part. H.G., C.W., and S.X. conducted the device characterization and demos. J.C., H.G., and Z.W. helped draw the design sketches. X.X. and Z.L.W. guided the project. W.D., J.Z., X.X., and Z.L.W. analyzed the data and prepared the manuscript. J.Z. acknowledges the support from NWRI-BioLargo Graduate Fellowship.

Conflict of Interest

The authors declare no conflict of interest.

Keywords

hand-powered pumps, triboelectric nanogenerators, water disinfection

Received: April 23, 2019

Revised: May 22, 2019

Published online:

- [1] World Health Organization, Progress on Drinking Water, Sanitation and Hygiene: 2017 Update and SDG Baselines, World Health Organization (WHO) and the United Nations Children's Fund (UNICEF), Geneva 2017.
- [2] M. R. Schock, R. N. Hyland, M. M. Welch, *Environ. Sci. Technol.* **2008**, *42*, 4285.
- [3] F. M. Burkle, P. G. Greenough, *Disaster Med. Public* **2008**, *2*, 192.
- [4] M. Boller, *Water Sci. Technol.* **1997**, *35*, 1.
- [5] M. D. Sobsey, C. E. Stauber, L. M. Casanova, J. M. Brown, M. A. Elliott, *Environ. Sci. Technol.* **2008**, *42*, 4261.
- [6] B. W. Lykins, *Point-of-Use/Point-of-Entry for Drinking Water Treatment: 0*, CRC Press, Boca Raton, Florida 2018.
- [7] B. F. Arnold, J. M. Colford Jr., *Am. J. Trop. Med. Hyg.* **2007**, *76*, 354.
- [8] R. L. Wolfe, *Environ. Sci. Technol.* **1990**, *24*, 768.
- [9] M. Mukherjee, Y. Hu, C. H. Tan, S. A. Rice, B. Cao, *Sci. Adv.* **2018**, *4*, eaau1459.
- [10] S.-L. Loo, A. G. Fane, T.-T. Lim, W. B. Krantz, Y.-N. Liang, X. Liu, X. Hu, *Environ. Sci. Technol.* **2013**, *47*, 9363.
- [11] A. S. Adeleye, J. R. Conway, K. Garner, Y. Huang, Y. Su, A. A. Keller, *Chem. Eng. J.* **2016**, *286*, 640.
- [12] C. Liu, D. Kong, P.-C. Hsu, H. Yuan, H.-W. Lee, Y. Liu, H. Wang, S. Wang, K. Yan, D. Lin, *Nat. Nanotechnol.* **2016**, *11*, 1098.
- [13] X. Mao, W. Tian, Y. Ren, D. Chen, S. E. Curtis, M. T. Buss, G. C. Rutledge, T. A. Hatton, *Energy Environ. Sci.* **2018**, *11*, 2954.
- [14] Z.-Y. Huo, J.-F. Zhou, Y. Wu, Y.-H. Wu, H. Liu, N. Liu, H.-Y. Hu, X. Xie, *J. Mater. Chem. A* **2018**, *6*, 18813.
- [15] J. Plazas-Tuttle, D. Das, I. V. Sabaraya, N. B. Saleh, *Environ. Sci.: Nano* **2018**, *5*, 72.
- [16] H. Gómez-Couso, M. Fontán-Sainz, K. G. McGuigan, E. Ares-Mazás, *Acta Trop.* **2009**, *112*, 43.
- [17] C. A. Martínez-Huitle, E. Brillas, *Angew. Chem., Int. Ed.* **2008**, *47*, 1998.
- [18] Y. Chang, D. Reardon, P. Kwan, G. Boyd, J. Brant, K. Rakness, D. Furukawa, *Evaluation of Dynamic Energy Consumption of Advanced Water and Wastewater Treatment Technologies*, AWWA Research Foundation, Denver 2008.
- [19] M. A. Massoud, A. Tarhini, J. A. Nasr, *J. Environ. Manage.* **2009**, *90*, 652.
- [20] F.-R. Fan, Z.-Q. Tian, Z. Lin Wang, *Nano Energy* **2012**, *1*, 328.
- [21] Z. L. Wang, *Nature* **2017**, *542*, 159.
- [22] K. Dong, J. Deng, W. Ding, A. C. Wang, P. Wang, C. Cheng, Y.-C. Wang, L. Jin, B. Gu, B. Sun, Z. L. Wang, *Adv. Energy Mater.* **2018**, *8*, 1801114.
- [23] K.-W. Lim, M. Peddigari, C. H. Park, H. Y. Lee, Y. Min, J.-W. Kim, C.-W. Ahn, J.-J. Choi, B.-D. Hahn, J.-H. Choi, D.-S. Park, J.-K. Hong, J.-T. Yeom, W.-H. Yoon, J. Ryu, S. N. Yi, G.-T. Hwang, *Energy Environ. Sci.* **2019**, *12*, 666.
- [24] X. Pu, H. Guo, J. Chen, X. Wang, Y. Xi, C. Hu, Z. L. Wang, *Sci. Adv.* **2017**, *3*, e1700694.
- [25] A. Li, Y. Zi, H. Guo, Z. L. Wang, F. M. Fernández, *Nat. Nanotechnol.* **2017**, *12*, 481.
- [26] J. Cheng, W. Ding, Y. Zi, Y. Lu, L. Ji, F. Liu, C. Wu, Z. L. Wang, *Nat. Commun.* **2018**, *9*, 3733.
- [27] G. Q. Gu, C. B. Han, C. X. Lu, C. He, T. Jiang, Z. L. Gao, C. J. Li, Z. L. Wang, *ACS Nano* **2017**, *11*, 6211.
- [28] S. Chen, C. Gao, W. Tang, H. Zhu, Y. Han, Q. Jiang, T. Li, X. Cao, Z. Wang, *Nano Energy* **2015**, *14*, 217.
- [29] S. Chen, N. Wang, L. Ma, T. Li, M. Willander, Y. Jie, X. Cao, Z. L. Wang, *Adv. Energy Mater.* **2016**, *6*, 1501778.
- [30] Y. Long, Y. Yu, X. Yin, J. Li, C. Carlos, X. Du, Y. Jiang, X. Wang, *Nano Energy* **2019**, *57*, 558.
- [31] Q. Jiang, Y. Jie, Y. Han, C. Gao, H. Zhu, M. Willander, X. Zhang, X. Cao, *Nano Energy* **2015**, *18*, 81.
- [32] J. Tian, H. Feng, L. Yan, M. Yu, H. Ouyang, H. Li, W. Jiang, Y. Jin, G. Zhu, Z. Li, Z. L. Wang, *Nano Energy* **2017**, *36*, 241.
- [33] J. Zhou, T. Wang, X. Xie, *Environ. Int.* **2019**, *128*, 30.
- [34] G. Zhu, J. Chen, T. Zhang, Q. Jing, Z. L. Wang, *Nat. Commun.* **2014**, *5*, 3426.
- [35] A. Ahmed, I. Hassan, T. Ibn-Mohammed, H. Mostafa, I. M. Reaney, L. S. C. Koh, J. Zu, Z. L. Wang, *Energy Environ. Sci.* **2017**, *10*, 653.